

STUDY OF AN AQUEOUS LITHIUM CHLORIDE DESICCANT SYSTEM PART II: DESICCANT REGENERATION

Nelson Fumo

Departamento de Ingeniería Mecánica, Universidad Nacional Experimental del Táchira, San Cristóbal, Venezuela.
Telefax: (58-76) 532454, E-Mail: nfumo@telcel.net.ve

Yogi Goswami¹

Mechanical Engineering Department, University of Florida, 220 MEB, PO Box 116300, Gainesville, FL 32611-6300, USA
Tel.: (352) 392-0812, Fax: (352) 392-1071, E-Mail: solar@cinnar.me.ufl.edu

ABSTRACT

Desiccant systems have been proposed as alternative to handle the latent load in vapor compression air conditioning for energy saving. The air dehumidification occurs because of the difference in vapor pressure which let the moisture diffuse from the air to the liquid desiccant. The diffused moisture cause a dilution of the desiccant which must be regenerated to return it to the original conditions. This paper presents the results from a study of the performance of a packed tower regenerator for an aqueous lithium chloride desiccant dehumidification system. The rate of water evaporation, as well as the effectiveness of the regeneration process were assessed under the effects of variables such as air and desiccant flow rates, air temperature and humidity, and desiccant temperature and concentration. A variation of the Öberg and Goswami mathematical model was used to predict the experimental findings given satisfactory results.

Keywords: Liquid desiccant, regeneration, lithium chloride, packed tower, regenerator, desiccant cooling.

INTRODUCTION AND BACKGROUND

Conventional vapor compression air conditioning systems are designed to handle the sensible and latent loads to provide conditions for human thermal comfort. The latent load is related to a moisture, and has associated the called air dehumidification process. For air dehumidification it is necessary cool down the air below its dew point in order to condense the moisture from the air, and reduce the air humidity to the desired value. This process requires a great amount of energy. Because a liquid desiccant system can handle the latent load by means of a negligible pump energy consumption, liquid desiccant cooling systems have become an alternative of great interest for HVAC industry.

Any liquid desiccant cooling system has two main components, the dehumidifier or absorber, and the regenerator. In our previous paper "Study of an Aqueous Lithium Chloride Desiccant System. Part I: Air Dehumidification" were presented experimental and theoretical results from a packed bed dehumidifier. The moisture that diffuses from the air to the liquid desiccant cause a dilution of the desiccant resulting in a reduction of its ability to absorb water. Therefore, the desiccant must be regenerated to give it back the original concentration. The regeneration process requires heat which can be obtained from a low pressure low temperature source, for which solar energy and waste energy from other

process are suitable. Different ways to regenerate liquid desiccants have been proposed. Hollands [1963] presented the result from the regeneration of lithium chloride in a solar still. Hollands focuses his study in the still efficiency, concluding that lithium chloride can be regenerated in a solar still with a daily efficiency of 5 to 20% depending on the insolation and the concentration of the desiccant. Ahmed et al [1998] presented the exergy analysis of a partly closed solar regenerator to be compared with the solar collector previous reported. Ahmed et al [1997] simulated a hybrid cycle with partly closed-open solar regenerator for regenerating the weak solution. They found that the system COP is about 50% higher than that of a conventional vapor absorption machine. Lebouf and Löf [1980] presented the analysis of a lithium chloride open cycle absorption air conditioner which utilizes a packed bed for regeneration of the desiccant solution driven by solar heated air. In this case, the air temperature ranges from 65°C to 96°C while the desiccant temperature ranges from 40°C to 55°C. Löf et al [1984] conducted an experimental and theoretical studied of the regeneration of aqueous lithium chloride solutions in a packed column supplied with solar heated air. In this case, air at temperature of 82°C to 109°C was used to regenerate the desiccant at an average temperature of 36°C. Öberg and Goswami [1998] justified the use of packed beds as the equipment for mass transfer when liquid desiccant are used. As a continuation of Öberg and Goswami [1998] study, and our previous report, this paper present the results from an experimental and theoretical study of the regeneration of an aqueous lithium chloride solution in a packed tower. For a constant tower height of 0.6 m, the rate of water evaporation from the desiccant was studied experimentally as a function of the following variables: air and desiccant flow rates; air temperature and humidity ratio; and desiccant temperature and concentration. For the same variables an analysis of the tower efficiency was done through the humidity effectiveness.

EXPERIMENTAL FACILITY AND PROCEDURE

A schematic of the experimental facility is shown in Fig. 1. The packed bed absorption tower was constructed from a 25.4 cm (24 cm ID) diameter acrylic tube to allow for flow visualization. The height of the tower is constant and equal to 60 cm. The packing used was 2.45 cm (1 in) polypropylene Rauschert Hiflow® rings with specific surface area of 210 m²/m³. Fresh, unused lithium chloride was stored in a tank, and its temperature was adjusted by circulating cold or warm water through a submerged stainless

¹ Author to whom all correspondence should be addressed.

coil. Air was blown past an air heater or a cooling coil, and through a humidifying chamber to adjust its temperature and relative humidity before it enters the packed tower. When the desired air and desiccant conditions were obtained, the desiccant was allowed to flow through the tower. The desiccant was distributed over the packing by three spray heads evenly spaced in an equilateral triangular configuration. Once steady state was obtained, measurements were taken using a PC-based data acquisition system. These measurements included inlet and outlet temperatures of the desiccant and the air using copper-constantan thermocouples, as well as inlet and outlet air relative humidities using humidity probes. In addition, samples of the desiccant

entering the dehumidifier were taken during the experiment and analyzed for water content using Karl Fischer titration. The rate of water evaporation from the liquid desiccant was studied experimentally as a function of the following variables: air and desiccant flow rates; air temperature and humidity ratio; and desiccant temperature and concentration. For the same variables an analysis of the tower efficiency was done using humidity effectiveness. Experiments were conducted for each variable at three levels (low, intermediate, and high value) while keeping the other variables constant. Three experiments were conducted at each level, and an average was used in the results.

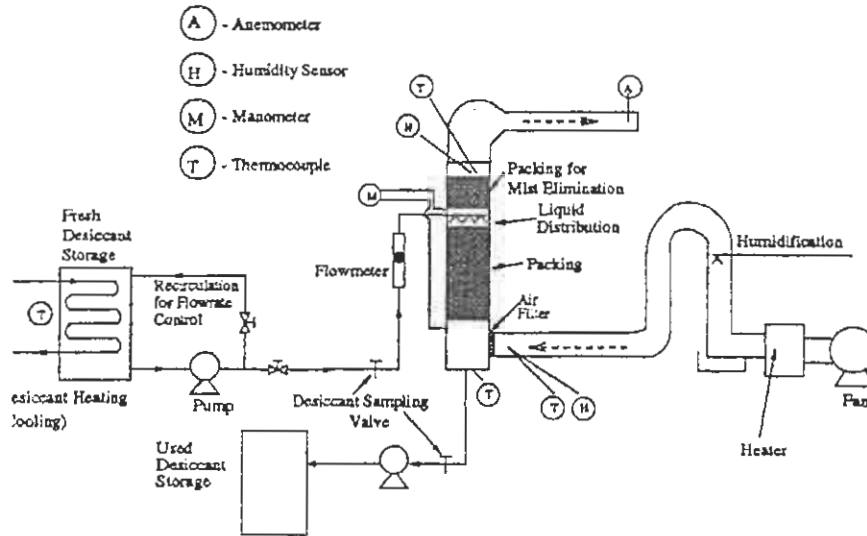


Fig. 1 Experimental facility.

THEORETICAL MODEL OF THE PACKED BED ABSORPTION TOWER

Öberg and Goswami [1998b] developed a finite difference model based on the model for adiabatic gas absorption presented by Treybal (1969) with the exception that the resistance to heat transfer in the liquid phase was neglected. For their model they assumed adiabatic absorption; concentration and temperature gradients in the flow direction (Z-direction, referring to Fig. 2) only water is transferred between the air and the desiccant, for their case; the interfacial surface area is the same for heat transfer and mass transfer, and equal to the specific surface area of the packing; the heat of mixing is negligible as compared to the latent heat of condensation of the water; and the resistance to heat transfer in the liquid phase is negligible. For the finite difference model, the packed bed height Z is divided into small segments, dZ (Fig. 2b), and the mass and energy balances are solved for each segment, from the bottom to the top of the tower. Since only the inlet conditions of the desiccant are known, the outlet conditions must initially be guessed, and iterations are required to find the desiccant outlet conditions that give the known inlet conditions at the top of the packed bed.

Öberg and Goswami's finite difference model required two modifications to account for the higher surface tension of LiCl and higher water concentration in brines as compared to water concentration in TEG. The modifications and governing equations

that describe the change in air humidity and air temperature, desiccant temperature and desiccant concentration, and desiccant flow rate across a segment are given below.

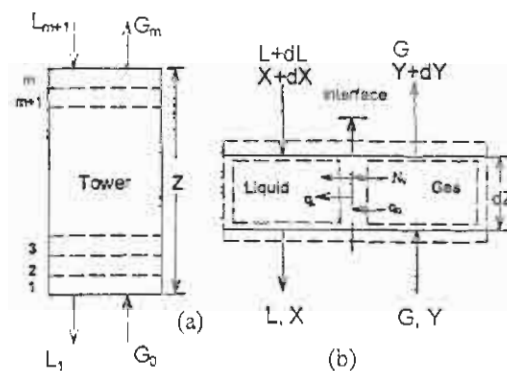


Fig. 2 Packed bed: (a) overview; (b) differential segment

Öberg and Goswami assumed that the interfacial surface area is the same for heat and mass transfer, and is equal to the specific surface area of the packing. Because of the high surface tension of LiCl solutions, twice that of glycol, the packing is wetted

insufficiently causing a considerable reduction of the area for mass transfer. Therefore, to estimate the wet area, an equation for wetted surface area proposed by Onda et al (1968) was used:

$$\frac{a_w}{a_t} = 1 - \exp \left[-1.45 \left(\frac{\gamma_L}{\rho_L} \right)^{0.75} \left(\frac{L}{a_t \cdot \mu_L} \right)^{0.1} \left(\frac{L^2 \cdot a_t}{\rho_L^2 \cdot g} \right)^{-0.05} \left(\frac{L^2}{\rho_L \cdot \gamma_L \cdot a_t} \right)^{0.2} \right] \quad (1)$$

This equation takes into account the liquid surface tension and the surface energy of packing materials, and was used by Öberg and Goswami in the definition of the k-Type mass transfer coefficients²:

$$k_L = 0.0051 \left(\frac{\mu_L \cdot g}{\rho_L} \right)^{1/3} \left(\frac{L}{a_w \cdot \mu_L} \right)^{2/3} \left(\frac{\rho_L \cdot D_L}{\mu_L} \right)^{1/2} (a_t \cdot D_p)^{0.4} \quad (2)$$

$$k_G = 5.23 \frac{a_t \cdot D_G}{R \cdot T_a} \left(\frac{G}{a_t \cdot \mu_G} \right)^{0.7} \left(\frac{\mu_G}{\rho_G \cdot D_G} \right)^{1/3} (a_t \cdot D_p)^{-2} \quad (3)$$

Then, the change in air humidity across the differential segment is defined by:

$$\frac{dY}{dZ} = - \frac{M_w \cdot F_G \cdot a_w}{G} \cdot \ln \left(\frac{1-y_i}{1-y} \right) \quad (4)$$

Where the interfacial gas phase concentration is given by:

$$y_i = 1 - (1-y) \cdot \left(\frac{x}{x_i} \right)^{\frac{F_L}{F_G}} \quad (5)$$

Equation (5) was used with the vapor-liquid equilibrium curve for LiCl to solve for the interfacial concentrations in the gas and liquid phases.

The k-Type mass transfer coefficients for liquid phase can be converted to F-Type coefficients by:

$$F_L = k_L \cdot x_{SM} \cdot \frac{\rho_L}{M_L} \quad (6)$$

Where x_{SM} may be considered equal to 1 for very dilute solutions. For lithium chloride the logarithmic mean desiccant mole fraction difference between the bulk liquid and interface values must be calculated as:

$$x_{SM} = \frac{x - x_i}{\ln \left(\frac{x}{x_i} \right)} \quad (7)$$

The k-Type mass transfer coefficient for gas phase can be converted to F-Type coefficients by:

$$F_G = k_G \cdot P \quad (8)$$

² As stated by Onda et al (1968), in equations 2 and 3, D_p represents the nominal size of the packing.

The change in air temperature across the differential segment is given by:

$$\frac{dT_a}{dZ} = \frac{h'_G a_t \cdot (T_L - T_a)}{G \cdot (c_{p,a} + Y \cdot c_{p,v})} \quad (9)$$

Where $h'_G a_t$ is the heat transfer coefficient corrected for simultaneous heat and mass transfer:

$$h'_G a_t = \frac{-G \cdot c_{p,v} \cdot \frac{dY}{dZ}}{1 - \exp \left(\frac{G \cdot c_{p,v} \cdot \frac{dY}{dZ}}{h_G \cdot a_t} \right)} \quad (10)$$

Applying the heat and mass transfer analogy, it is found that the gas phase heat transfer coefficient is:

$$h_G = F_G \cdot M_a \cdot (c_{p,a} + Y \cdot c_{p,v}) \cdot \frac{Sc^{2/3}}{P_r^{2/3}} \quad (11)$$

With Schmidt number $Sc = \frac{\mu_G}{\rho_G \cdot D_G}$.

The change in desiccant flow rate, concentration and temperature across the differential segment are given by equations 12, 13 and 14 respectively:

$$\frac{dL}{dZ} = G \cdot \frac{dY}{dZ} \quad (12)$$

$$\frac{dX}{dZ} = - \frac{G}{L} \cdot X \cdot \frac{dY}{dZ} \quad (13)$$

$$\frac{dT_L}{dZ} = \frac{G}{c_{p,L} \cdot L} \left\{ (c_{p,a} + Y \cdot c_{p,v}) \frac{dT_a}{dZ} + [c_{p,v} \cdot (T_a - T_o) - c_{p,L} (T_L - T_o) + \lambda_o] \frac{dY}{dZ} \right\} \quad (14)$$

Vapor pressure is an important property which determines the air humidity ratio in equilibrium with the desiccant at the interface. In this study a second order polynomial was used and the coefficients were obtained from a curve fit using data from Uemura (1967):

$$p_v = (a_0 + a_1 \cdot T + a_2 \cdot T^2) + (b_0 + b_1 \cdot T + b_2 \cdot T^2) \cdot X + (c_0 + c_1 \cdot T + c_2 \cdot T^2) \cdot X^2 \quad (15)$$

$a_0=16.294$, $a_1=-0.8893$, $a_2=0.01927$ $b_0=74.3$
 $b_1=-1.8035$, $b_2=-0.01875$ $c_0=-226.4$, $c_1=7.49$
 $c_2=-0.039$; T (°C), X (kg_L:C/kg_S:S).

The efficiency of the tower was evaluated through a humidity effectiveness defined as:

$$\epsilon_y = \frac{Y_{OUT} - Y_{IN}}{Y_{equ} - Y_{IN}} \quad (16)$$

For this relation, Y_{IN} and Y_{OUT} , are the humidity ratios of the air at the inlet and outlet of the tower, respectively. Y_{equ} is the humidity ratio of the air, which is in equilibrium with the desiccant solution at the local solution temperature and concentration.

An additional consideration was introduced in the model to account for the non-uniform liquid distribution at the top of the tower. The packing volume that is dry is estimated by using geometric relations allowing the calculation of a correction factor for unwetted packing fraction, CF. This correction factor was used to modify the relation a_w/a_s in equation (1), by $a_w/(a_s \cdot CF)$.

RESULTS AND DISCUSSION

Table 1 present the experimental results, while figures 3 to 8 shows the experimental results together with the theoretical modeling. Uncertainties of the experimental measurements were calculated using the method by Kline and McClintock [1953]. It is seen from the figures that the adapted finite difference model shows very good agreement with the experimental findings. Figures 3 to 8 show that the influence of these variables may be assumed linear. Therefore, the slope of the evaporation rate curve (% change in m_{evap} / % change in variable) in these figures gives an estimation of the influence of these variables on the water evaporation rate. The water evaporation rate increases with the air flow rate with slope of 0.5 (Fig. 3). Since a high air flow rate rapidly removes the higher moist air from the interface, it reduces the humidity gradient between the interface and bulk air, maintaining a higher potential for mass transfer. The water evaporation rate increase with the inlet desiccant temperature with slope of 5 (Fig. 7). Since vapor pressure of the desiccant is highly dependent on the temperature, the higher the temperature the higher the vapor pressure, and consequently higher the potential for mass transfer. The water evaporation rate decreases with the inlet desiccant concentration with slope of -1.8 (Fig. 8). This may be explained from the fact that vapor pressure of the desiccant is a function of the concentration. Therefore, the higher the concentration, the lower the vapor pressure, and consequently lower the potential for mass transfer. The water evaporation rate

decreases with the inlet air humidity ratio with slope of -0.3 (Fig. 5). As expected, a higher humidity ratio implies higher air vapor pressure and consequently lower potential for mass transfer. The water evaporation rate increases with the desiccant flow rate with slope of 0.3 (Fig. 6). At higher desiccant flow rates there will be less reduction of the liquid temperature, maintaining a higher potential for mass transfer. The air temperature does not cause significant variation in the water evaporation rate (Fig. 4).

Efficiency of the regenerator is more sensitive than the dehumidifier. For the range of the variables studied, humidity effectiveness for the regenerator varies between 71 and 87%. Two defined tendencies were noticed from the results. One tendency is the apparent linear decrease of the humidity effectiveness for an increase in the air flow rate. This can be explained because for a higher air flow rate the air will be in contact with the liquid for a shorter period of time, giving a lower change in air humidity ratio (Fig. 9). The second defined tendency is the apparent linear increase of humidity effectiveness with the increase of desiccant flow rate. This can be explained from the result seen earlier that the water evaporation rate is proportional to the desiccant flow rate. Therefore, for a higher desiccant flow rate, the change in air humidity ratio will be higher (Fig. 10).

CONCLUSIONS

Reliable sets of data for lithium chloride regeneration were obtained. The influence of the design variables studied on the water evaporation rate can be assumed linear. Therefore, the slope of the evaporation rate curve in Figures 3 to 8 gives a measurement of the impact of the variables on the water evaporation rate. Design variables found to have the greatest impact on the performance of the regenerator are: desiccant temperature (slope, $m=5$), desiccant concentration ($m=-1.8$), air flow rate ($m=0.5$). The other variables have a slope equal or lower than 0.3. In this study the mass ratio of air to desiccant solution (MR) varied between 0.15 to 0.25 which is the same range used for air dehumidification experiments, and which is lower than the MR values of 1.3 to 3.3 used in most other studies. The adapted finite difference model shows very good agreement with the experimental findings

Table 1: EXPERIMENTAL RESULTS

G	INLET					OUTLET				m_{cond}
	T_a	Y	L	TL	X	T_a	Y	TL	X	
0.833	30.4	0.0183	6.463	65.0	34.0	58.9	0.0579	58.6	34.5	1.55
1.098	30.1	0.0180	6.206	65.1	34.1	59.3	0.0532	57.8	34.8	1.81
1.438	29.8	0.0177	6.479	65.1	34.5	57.5	0.0488	56.6	35.2	2.10
1.097	35.1	0.0180	6.349	65.1	33.4	58.5	0.0551	57.4	34.1	1.91
1.102	40.0	0.0178	6.354	65.0	33.6	58.9	0.0548	57.6	34.2	1.91
1.132	30.2	0.0143	6.370	65.2	34.0	57.6	0.0513	57.2	34.7	1.97
1.097	29.4	0.0210	6.440	65.5	33.6	58.5	0.0541	58.3	34.2	1.70
1.116	30.3	0.0182	5.185	65.4	34.4	57.6	0.0507	57.0	34.9	1.71
1.101	29.9	0.0180	7.541	65.2	34.3	59.0	0.0556	57.9	34.9	1.95
1.111	30.0	0.0187	6.245	60.3	34.4	55.8	0.0447	54.2	34.8	1.36
1.084	29.7	0.0184	6.315	70.0	34.5	62.6	0.0666	60.0	35.3	2.45
1.099	29.7	0.0177	6.400	64.8	32.8	57.6	0.0542	56.8	33.4	1.89
1.116	30.3	0.0182	6.428	65.0	34.9	57.9	0.0501	57.5	35.4	1.67

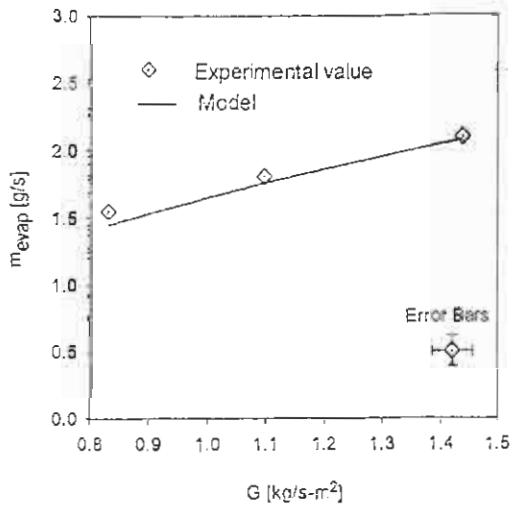


Fig 3: Influence of air flow rate

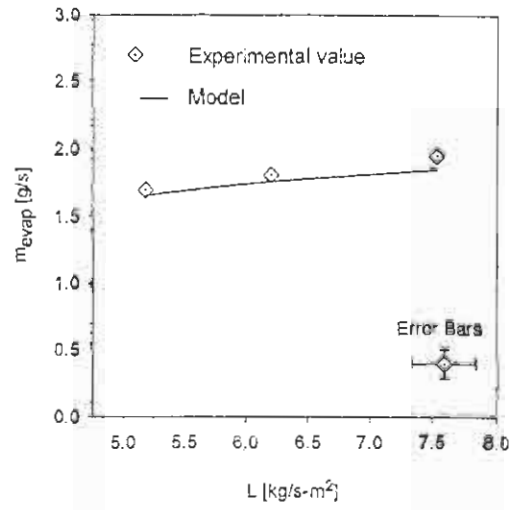


Fig. 6: Influence of desiccant flow rate

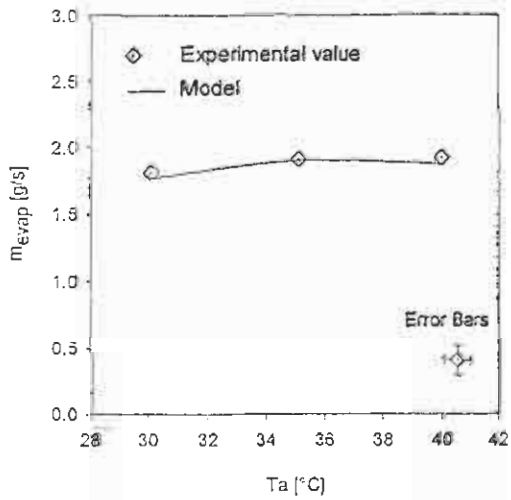


Fig. 4: Influence of inlet air temperature

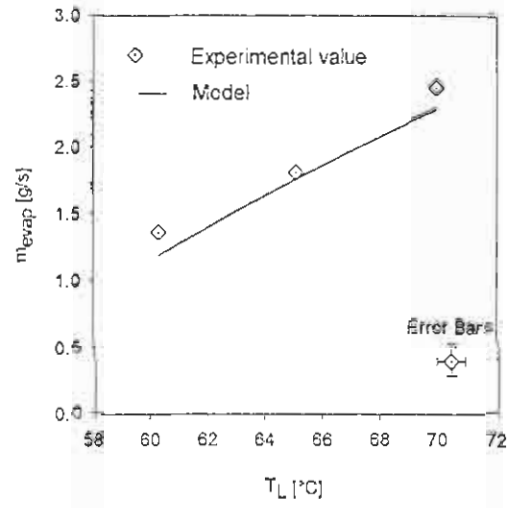


Fig. 7: Influence of inlet desiccant temperature

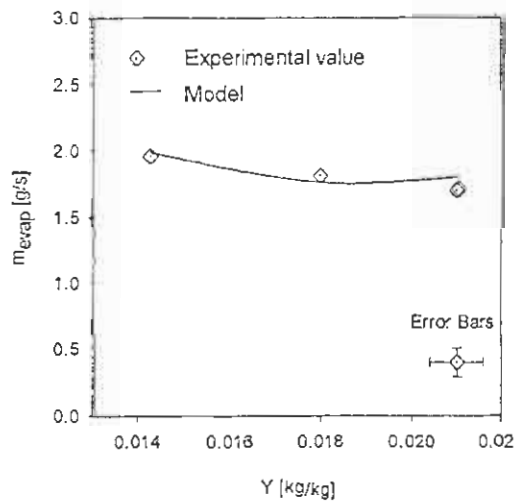


Fig. 5: Influence of inlet air humidity ratio

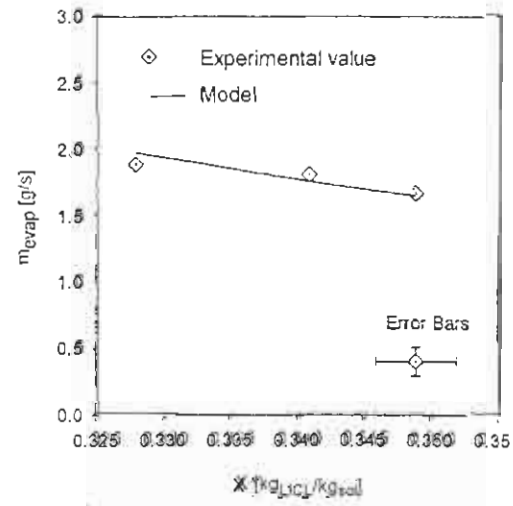


Fig. 8: Influence of inlet desiccant concentration

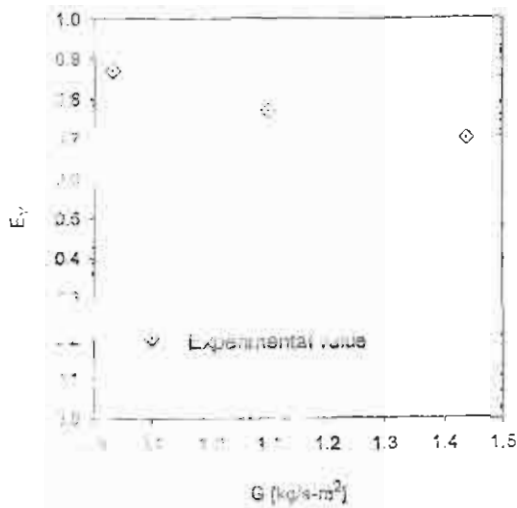


Fig. 9: Influence of air flow rate on humidity effectiveness

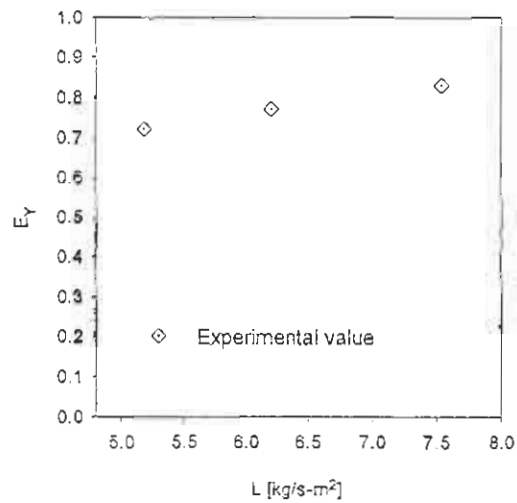


Fig. 10: Influence of desiccant flow rate on humidity effectiveness

NC	nominal size of packing (m)
a	specific surface area of packing (m ² /m ³)
a _w	wetted surface area of packing (m ² /m ³)
c _p	specific heat (kJ/kg-°C)
D	diffusivity (m ² /s)
D _p	nominal size of packing (m)
F _G	gas phase mass transfer coefficient (kmol/m ² -s)
F _L	liquid phase mass transfer coefficient (kmol/m ² -s)
G	air flow rate (kg/m ² -s)
g	acceleration of gravity (m/s ²)
h _G	gas phase enthalpy transfer coefficient (kJ/m ² -s)
k _G	gas phase mass transfer coefficient (kmol/m ² -s-Pa)
k _L	liquid phase mass transfer coefficient (m/s)
L	superficial desiccant flow rate (kg/m ² -s)
LiCl	lithium chloride
M	molar mass (kg/kmol)
m	flow rate (g/s) or (kg/s)
p	pressure (Pa)
p _{atm}	atmospheric pressure (Pa)
Sc	Schmidt number
T	temperature (°C)
TEG	triethylene glycol
X	desiccant concentration (kg _{LiCl} / kg _{solution})
x	desiccant mole fraction (kmol _{LiCl} / kmol _{solution})
x _{b,liq}	equilibrium solvent mole fraction difference between the bulk liquid and interface values (kmol _{LiCl} / kmol _{solution})
Y	air humidity ratio (kg water/kg dry air)
y	water mole fraction (kmol water / kmol air)
Z	tower height (m)
γ	surface tension (N/m)
ε	effectiveness
λ	latent heat of condensation (kJ/kg)
ν	viscosity (N/m ²)
ρ	density (kg/m ³)
ρ _{abs}	absorbance
τ	time (s)

c	= critical
cond	= water condensation
equ	= equivalent
G	= gas phase
IN	= inlet
i	= interface
L	= desiccant or liquid phase
OUT	= outlet
o	= reference state

REFERENCES

- Ahmed Khalid C. S., Gandhidasan P., Zubair S. M., and Al-Farayedhi A. A., 1997, "Simulation of a Hybrid Liquid Desiccant Based Air-Conditioning System", *Applied Thermal Engineering*, Vol. 17, No. 2, pp. 125-134.
- Ahmed Khalid C. S., Gandhidasan P., Zubair S. M., and Al-Farayedhi A. A., 1998, "Exergy Analysis of a Liquid Desiccant Based Air-Conditioning System", *Energy*, Vol. 23, No. 1, pp. 51-59.
- Hollands K. G. T., 1963, "The Regeneration of Lithium Chloride Brine in a Solar Still", *Solar Energy*, Vol. 7, No. 2, pp. 39-43.
- Kline S. J., and McClinton F. A., 1953, "Uncertainties in Single-Sample Experiments.", *Mechanical Engineering*, Vol. 75, pp. 3-8.
- Leboeuf Cecile M., and Löf George O. G., 1980, "Open-Cycle Absorption Cooling Using Packed-Bed Absorbent Reconcentration", *Proceedings of the Annual Meet American Sectional International Solar Energy Society AS/ISES*, Vol. 3, No. 1., pp. 205-209.
- Löf G. O. G., Lenz T. G. And Rao S., 1984, "Coefficients of Heat and Mass Transfer in a Packed Bed Suitable for Solar Regeneration of Aqueous Lithium Chloride Solutions", *Journal of Solar Energy Engineering*, Vol. 106, pp. 387-392.
- Öberg Viktoria, and Goswami D. Yogi, 1998, "Experimental Study of the heat and mass Transfer in a Packed Bed Liquid Desiccant Air Dehumidifier", *Solar Engineering International Solar Energy Conference*, ASME, NJ, pp. 155-166.